Int J Thermophys (2010) 31:987–997
DOI 10.1007/s10765-010-0763-3

# Diffusion of Methylene Blue in Phantoms of Agar Using a Photoacoustic Technique

**L. Vilca-Quispe · J. J. Alvarado-Gil · P. Quintana · J. Ordonez-Miranda**

Received: 18 June 2009 / Accepted: 18 May 2010 / Published online: 20 June 2010


**Abstract** In this work, the kinetics of diffusion of methylene blue in agar aqueous solution is studied using a photoacoustic technique. Two agar phantoms solutions in water with a relation of mass/volume of 0.01 % and 0.05 % were analyzed. The study was performed using a modified Rosencwaig photoacoustic cell that is enclosed by transparent windows, on both sides. The sample is deposited directly on top of the upper window. A red light beam, at a fixed modulation frequency, is sent through the lower window illuminating the sample and inducing the photoacoustic effect inside the closed chamber of the cell. At the beginning of the experiment, a droplet of 100 μL of agar solution is deposited; afterwards, the signal stabilizes, and 10 μL of methylene blue aqueous solution ($0.0125\,\mathrm{g}\cdot\mathrm{mL}^{-1}$) is added to the surface of the agar. During the first seconds of the experiment, the photoacoustic signal amplitude increases followed by a gradual and long decay. Results for modulation frequencies in the range from 10 Hz to 80 Hz for both agar concentrations are presented. A simple theoretical approach is presented to analyze the experimental data. It is demonstrated that the kinetics of the process can be parameterized as a function of the changes of an effective optical absorption coefficient. From these results, the characteristic time, in which the dye diffusion process stabilizes, is obtained. It is found that this time is larger for samples with a higher agar concentration. These differences provide important results for biomedical sciences in which agar gels are used as phantoms resembling some of the properties of living organs and tissues.

L. Vilca-Quispe · J. J. Alvarado-Gil (✉) · P. Quintana · J. Ordonez-Miranda
Applied Physics Department, CINVESTAV-IPN Unidad Mérida, Carretera Antigua a Progreso km. 6, Col. Gonzalo Guerrero, CP 97310, Merida, Yucatan, México
e-mail: jjag09@yahoo.com

**Keywords** Agar phantom · Composite materials · Diffusion · Methylene blue · Modified potoacoustic cell

## 1 Introduction

Diffusion of substances in tissue is an extremely complex process. Various phantoms have been proposed as a model to simulate biological organs and to study physicochemical effects on the human body. Low concentration aqueous agar phantoms systems are specially suited for this purpose [1], because they resemble the desired tissue, and are cheap to prepare [2]. Recently, they have been suggested for the study of the treatment of neurodegenerative diseases of the central nervous system (CNS) by implantation of nanoreservoirs, for controlled drug release into the brain [3]. A variety of experimental methods have been developed as an alternative for the study of drug diffusion phenomena in such a complex system. Methylene blue can be used to monitor the diffusion processes inside a gel-like material to simulate the actual process occurring in the living tissue, since the size of this molecule is similar to that of some chemotherapeutic drugs [4].

Various techniques have been developed to study this kind of process using microscopy, optical techniques, electrical analysis, etc. [2]. For the experimenter, it is always important to have access to new, simple, and reliable methodologies. During the last few years, photoacoustic (PA) techniques have been demonstrated to be useful tools for materials characterization, and in the study of diverse phenomena [5–7]. PAs have been used recently in the study of the evolution of dynamic systems, such as oxygen release in plants, blood sedimentation, evaporation of liquids, etc. [8–11]. The PA signal is not only directly related to the time evolution of the optical and thermal properties, but also with various physical processes leading to modulated heat and additional changes in the geometry of the sample [12]. The PA technique is based on the periodic heating of a sample illuminated with modulated optical radiation. In a gas-microphone configuration, the sample is in contact with the gas-tight cell. In addition to a steady-state temperature gradient, a thermal wave in the material couples back to the gas around the sample and this will result in a periodic fluctuation of the temperature of a thin layer of gas, close to the sample surface. This thin layer of gas will act as an acoustic piston, which will result in the production of a periodic pressure change in the cavity. A sensitive microphone coupled to the sample chamber can be used to detect this pressure fluctuation.

In this work, the diffusion of an aqueous solution of methylene blue into an agar gel using PA spectroscopy is presented. The study was performed using a modified Rosencwaig PA cell [13,14], in which the sample is illuminated with a modulated red laser beam at a fixed frequency [15,16]. A simple theoretical analysis that allows the determination of the evolution of the effective optical properties as well as the stabilization time of the process is presented. It is shown that a characteristic time, in which the dye diffusion process stabilizes, can be obtained. The relationship of this parameter with agar concentration is discussed.

## 2 Materials and Methods

### 2.1 Materials Preparation

Samples were prepared at two concentrations of agar powder (BD Bioxon Higroscopic Bacteriologic Agar) and 17.4 MΩ · cm of de-ionized water. The following agar powder concentration in water is used [100 × mass of agar powder/(mass of agar powder + mass of water)] and fixed at 0.01 % and 0.05 % mass/volume (w/v). The mixture was heated to 80 °C in such a way that all the agar powder is completely dissolved; then the resulting solution was cooled to room temperature, and deposited in sealed containers.

### 2.2 Photoacoustic Technique

The diffusion process of methylene blue aqueous solutions in agar samples was analyzed by the PA technique. It consisted of a conventional PA cell (see Figs. 1 and 2), closed on one side by a transparent quartz window and on the other by a transparent polyvinyl acetate foil, with a thickness of 98 μm [17]. On top of this foil, the agar gel sample was deposited. The polyvinyl acetate sample was illuminated through the quartz transparent window. An electret microphone is used, coupled to the cavity wall, to detect the pressure fluctuations in the PA chamber, generated by the periodic light beam of a 160 mW diode laser at 658 nm (ML120G21) modulated at constant frequency. The microphone signal is fed into a lock-in amplifier (SR830), from where the output signal amplitude is recorded, as a function of time, in a personal computer. At the beginning of the experiment, 100 μL of agar solution are deposited; when the signal stabilizes, 10 μL of methylene blue solution ($0.0125\,\mathrm{g}\cdot\mathrm{mL}^{-1}$) are added to the surface of the agar with a micropipete. As a consequence of the methylene blue diffusion inside the agar, the PA signal changes in the subsequent stages. In order to get data independent of the microphone characteristics, the PA signal amplitude at any time was normalized dividing it by the maximum value of the PA signal amplitude for a given experiment.

### 2.3 Thermal Diffusivity Measurements

The thermal diffusivity of the agar samples for the two concentrations were measured using the thermal wave cavity technique [18,19]. The experimental setup consists of an aluminum cavity, in which the sample is deposited on top of a pyroelectric detector (110 μm thick polyvinyl dine fluoride film). The sample is enclosed on top by an aluminum foil that is illuminated with an IR diode laser (Sanyo DL-7140-201S at 785 nm and 70 mW). The laser was electronically modulated by the internal sine oscillator of the lock-in amplifier (SR-830) and controlled by a diode laser driver (Melles-Griot-06DLD205). The thermal wave generated on one of the surfaces of the cavity is transmitted through the sample, and detected on the other side by the pyrolectric detector. The generated signal is preamplified using a low noise preamplifier (SR-560) to improve the signal-to-noise ratio and to optimize the impedance coupling. Details of the thermal wave cavity (TWC) cell design and configuration

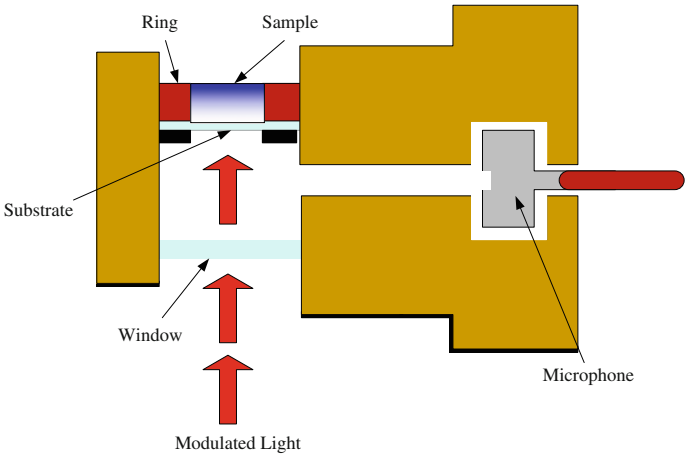


**Fig. 1** Schematic cross section of the used conventional PA cell

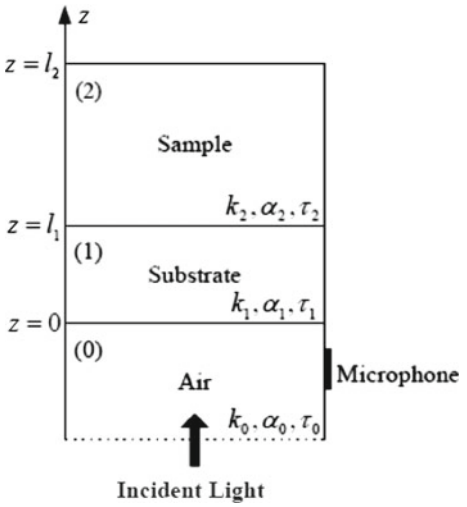


**Fig. 2** Cross-sectional view of a simple cylindrical photoacoustic cell, showing the positions of the agar gel sample, backing material, and gas column

have been previously reported in the literature [18]. In order to measure the thermal diffusivity, length scans of the thermal wave cavity were performed with a stepper motor coupled to a translation stage. All data acquisition and cavity length scans were automated with a home-made Lab-View® program.

## 2.4 Optical Measurements

In order to evaluate the changes in the optical properties of agar gel, a simple optical analysis was also performed to get a complementary description. This system consisted of a continuous red laser beam (657 nm) that was used to illuminate the sample inside a glass tube (10 cm × 3 mm) filled with a mixture of 96 μL of methylene blue

with agar. The methylene blue is added on top of the tube, and after that, the tube is turned upside down. Therefore, the methylene solution migrates inside the sample due to the difference in density. The decay in the transmitted light is a direct measurement of the changes in concentration and provides the parameters associated with the kinetic diffusion process.

## 3 Theory

In order to understand the evolution of the PA signal, a theoretical study of the modulated temperature is presented. To simplify the model, it is considered that the system has homogeneous optical and thermal properties at any given time.

The problem to be solved is to find the temperature inside the layered system shown in Fig. 1, using the heat conduction equation based on Fourier's law [20]:

$$\frac{\partial^2 T(z,t)}{\partial z^2} - \frac{1}{\alpha}\frac{\partial T(z,t)}{\partial t} = -\frac{S(z,t)}{k}, \tag{1}$$

where $z$ is the spatial coordinate, $t$ is the time, $T$ is the absolute temperature, $\alpha(k)$ is the thermal diffusivity (thermal conductivity) of the medium, and the heat source $S(z,t)$ is the rate per unit volume at which the heat flux is generated. In this case, the system is excited by a modulated temperature heat source at frequency $f$ of the form [5],

$$S(z,t) = F(z)\left(\frac{1+\cos(\omega t)}{2}\right) = \mathrm{Re}\left[\frac{F(z)}{2}\left(1+\mathrm{e}^{\mathrm{i}\omega t}\right)\right], \tag{2}$$

where $\omega = 2\pi f$, $\mathrm{Re}(\xi)$ is the real part of $\xi$, and $F$ is the spatial distribution of the deposited energy over the sample, per unit volume and unit time. For this heat source, the temperature at any point inside the sample ($z \geq 0$) is given by

$$T(z,t) = T_{\mathrm{amb}} + T_{\mathrm{dc}}(z) + T_{\mathrm{ac}}(z,t), \tag{3}$$

with $T_{\mathrm{amb}}$ being the ambient temperature. $T_{\mathrm{dc}}(z)$ and $T_{\mathrm{ac}}(z,t) = \mathrm{Re}\left[\theta(z)\mathrm{e}^{\mathrm{i}\omega t}\right]$ are the stationary raising and periodic components of the temperature, due to the first and second terms of the heat source, respectively. From now on, the operator $\mathrm{Re}\left[\theta(z)\mathrm{e}^{\mathrm{i}\omega t}\right]$ will be omitted, taking into account the convention that the real part of the expressions must be taken to obtain physical quantities. Our attention will be focused on the oscillatory part of the temperature, since it is the quantity of interest in lock-in and similar detection techniques.

Inserting Eqs. 2 and 3 into Eq. 1, and taking into account that $x$ and $t$ are mutually independent variables, then for $z \geq 0$, it is obtained that $\theta(z)$ satisfies the following differential equation:

$$\frac{\mathrm{d}^2\theta(z)}{\mathrm{d}z^2} - \sigma^2\theta(z) = -\frac{F(z)}{2k}, \tag{4}$$

where

$$\sigma = \sqrt{\frac{\mathrm{i}\omega}{\alpha}} = \frac{1+\mathrm{i}}{\mu}, \tag{5a}$$

$$\mu = \sqrt{\frac{2\alpha}{\omega}} = \sqrt{\frac{\alpha}{\pi f}}. \tag{5b}$$

Considering that layers 1 and 2 are excited by a laser light beam of periodically modulated intensity applied at the surface $z = 0$, the spatial heat source $F(z)$ inside these layers can be written as [5]

$$F_1(z) = \eta_1(1-R_1)I\beta_1\mathrm{e}^{-\beta_1 Z}, \tag{6a}$$

$$F_2(z) = \eta_2(1-R_2)\left[(1-R_1)I\mathrm{e}^{-\beta_1 l_1}\right]\beta_2\mathrm{e}^{-\beta_2 z}, \tag{6b}$$

where, for $j = 1, 2$, $\eta_j$ is the efficiency at which the absorbed light is converted into heat, $R_j$ is the surface reflection coefficient, $\beta_j$ is the absorption coefficient, and $I$ is the intensity of the light beam in the air for layer 0.

Assuming that the layers are in perfect thermal contact [21], the boundary conditions obtained from the usual requirement of temperature and heat flux continuity at the interfaces $z = 0, l_1$ are given by

$$\theta(z^-) = \theta(z^+), \tag{7a}$$

$$k(z^-)\frac{\mathrm{d}\theta(z^-)}{\mathrm{d}z} = k(z^+)\frac{\mathrm{d}\theta(z^+)}{\mathrm{d}z}, \tag{7b}$$

where the superscripts "+" and "−" indicate that the limit $z \to 0$ $(z \to l_1)$ is taken from the right and left of the point $z = 0$ $(\mathrm{z} = l_1)$, respectively.

Considering that layer 2 is sufficiently thick to avoid the presence of thermal waves traveling in the $-z$ direction inside it and using Eqs. 4–7, the following result is obtained for $z \leq 0$:

$$\theta(z) = \Theta\frac{\eta_1 r_1\left(\frac{\varepsilon_{21}+1}{r_1+1}\mathrm{e}^{\sigma_1 l_1} - \frac{\varepsilon_{21}-1}{r_1-1}\mathrm{e}^{-\sigma_1 l_1} + 2\frac{\varepsilon_{21}-r_1}{r_1^2-1}\mathrm{e}^{-\beta_1 l_1}\right) + 2(1-R_2)\frac{\eta_2 r_2}{r_2+1}\mathrm{e}^{-(\beta_1+\beta_2)l_1}}{(\varepsilon_{01}+1)(\varepsilon_{21}+1)\mathrm{e}^{\sigma_1 l_1} - (\varepsilon_{01}-1)(\varepsilon_{21}-1)\mathrm{e}^{-\sigma_1 l_1}}\mathrm{e}^{\sigma_0 z} \tag{8}$$

where $\sigma_m$ is defined by Eq. 5a for the thermal diffusivity of layer m = 0,1,2; and

$$\Theta = \frac{(1-R_1)I}{2\varepsilon_1\sqrt{\pi f}(1+\mathrm{i})}, \tag{9a}$$

$$\varepsilon_m = \frac{k_m}{\sqrt{\alpha_m}} \quad m = 0, 1, 2; \tag{9b}$$

$$\varepsilon_{mn} = \frac{\varepsilon_m}{\varepsilon_n} \quad m, n = 0, 1, 2; \tag{9c}$$

$$r_m = \frac{\beta_m}{\sigma_m} \quad m = 1, 2. \tag{9d}$$

Taking into account that under our experimental conditions, layer 1 can be considered as thermally thick and optically transparent ($\mu_1 << l_1 << 1/\beta_1$), $R_2 \approx 0$, which is a reasonable assumption for layer 2 (agar combined with methylene blue), $\eta_1 \approx \eta_2$ as usual [5], and $\beta_2 l_1 << 1$; Eq. 8 takes the form,

$$\theta(z) \approx \frac{\eta_1(1 - R_1)I\beta_1\sqrt{\alpha_1}}{4\pi i\varepsilon_1 f}\left(1 + T_{21}\sqrt{\alpha_{21}}\beta_{21}e^{-\sigma_1 l_1}\right)e^{\sigma_0 z}, \tag{10}$$

where $T_{21} = 2/(1 + \varepsilon_{21})$, $\beta_{21} = \beta_2/\beta_1$, and $\alpha_{21} = \alpha_2/\alpha_1$. It will be assumed that the thermal properties of layer 1 are fixed along the entire experiment and assuming that only the optical absorption coefficient $\beta_2$ of layer 2 is changing appreciably, during the process of diffusion of the methylene blue into the agar. This last assumption is valid for low concentrations of methylene blue only; it is convenient to define the normalized signal $\Omega$ as follows:

$$\Omega = \frac{\theta(z, \beta)}{\theta(z, \beta_0)} = \frac{\left(1 + T_{21}\sqrt{\alpha_{21}}\beta e^{-\sigma_1 l_1}\right)}{\left(1 + T_{21}\sqrt{\alpha_{21}}\beta_0 e^{-\sigma_1 l_1}\right)}, \tag{11}$$

where $\beta_0 = \beta_{21}(t = 0)$ is the normalized optical absorption coefficient at the beginning of the diffusion process and $\beta = \beta_{21}(t)$ is the normalized optical absorption coefficient at some subsequent time $t > 0$. After expressing the thermal signal in Eq. 11 as a complex function in its polar form, it can be shown that its amplitude $A(f)$ is given by

$$A(f) = \sqrt{\frac{1 + \left(T_{21}\sqrt{\alpha_{21}}\beta\right)^2 e^{-2\sqrt{f/f_c}} + 2T_{21}\sqrt{\alpha_{21}}\beta e^{-\sqrt{f/f_c}}\cos(\sqrt{f/f_c})}{1 + \left(T_{21}\sqrt{\alpha_{21}}\beta_0\right)^2 e^{-2\sqrt{f/f_c}} + 2T_{21}\sqrt{\alpha_{21}}\beta_0 e^{-\sqrt{f/f_c}}\cos(\sqrt{f/f_c})}}, \tag{12}$$

where $f_c = \alpha_1/\pi l_1^2$ is the cut-off frequency of layer 1. In this way, after determining experimentally the normalized amplitude given in Eq. 12, by means of a fitting procedure, the relative optical absorption coefficients $\beta$ can be determined for a fixed time during the diffusion process, if the thermal diffusivity and effusivity of layers 1 and 2 are known.

## 4 Results and Discussion

The time evolution of the PA signal for 0.01 % and 0.05 % w/v concentrations of agar phantoms are presented in Fig. 3a, b. It can be observed that in the first seconds the PA

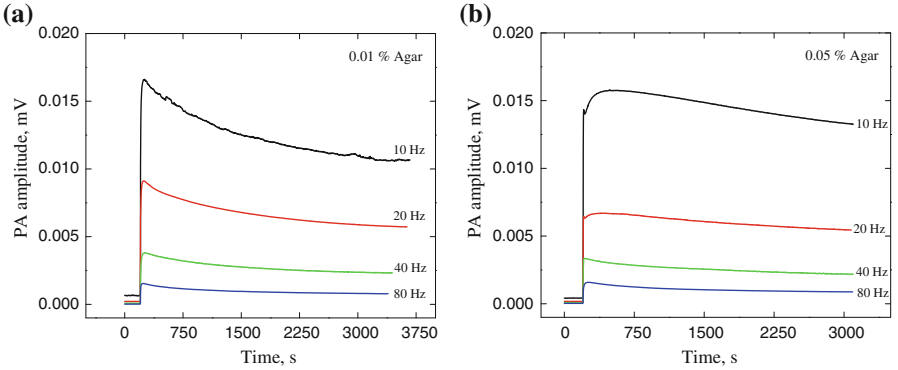


**Fig. 3** PA signal behavior as a function of time during the diffusion processes of the methylene blue through the solution, in (**a**) 0.01 % and (**b**) 0.05 % w/v, of agar phantoms

signal grows sharply, due to a sudden increase of the light absorption induced by the addition of the methylene blue solution. In a second stage, after 200 s, the PA signal decreases gradually, due to the progressive diffusion of the dye that induces a decrease of the light absorption. It can be observed that the signal for the sample with higher agar concentration shows a slower decay.

It is important to mention that the PA signal phase is shown to be highly susceptible to the initial conditions of the experiment, strongly dependent on the precise deposition procedure of the droplet of dye solution on top of the sample at such low agar concentrations. Therefore, although the phase of the PA signal presented adequate behavior for long times, this was not the situation for the first stage of the experiments. In contrast, the PA signal amplitude was shown to be less vulnerable to that process and therefore generated data that can be straightforwardly interpreted.

In Fig. 4a, b, the time dependence of the normalized signal amplitude is shown. These data were obtained dividing the PA signal by its maximum for the specific experiment. It can be observed that higher modulation frequencies are more sensitive to the changes induced by the diffusion process. It is important to mention that the normalization procedure is useful in making our results independent of the specific characteristics of the microphone and substrate; this is desirable if we want to focus our attention on the changes of the optical properties of the sample. This method also cancels the $1/f$ frequency dependence of the PA signal, leaving unaffected the frequency in the exponential terms. The effect of the normalization procedure, in fact, magnifies the observation of the dye diffusion process, without affecting the settle-down time and the net change of the signal. From the point of view of thermal wave theory, the thermal diffusion length is mainly related to the exponential decay. In this sense, the procedure of normalization is not canceling the most important dependence on the frequency that constitutes the basic advantage of PA spectroscopy.

Thermal diffusivities of the agar samples were measured using the thermal wave resonator cavity technique. The values for 0.01 % and 0.05 % w/v concentrations were $1.460\times10^{-7}$ $m^2\cdot s^{-1}$ and $1.466\times10^{-7}\,m^2\cdot s^{-1}$, respectively. These values are very close to the thermal diffusivity for pure water [5]. Additionally, the measurements of

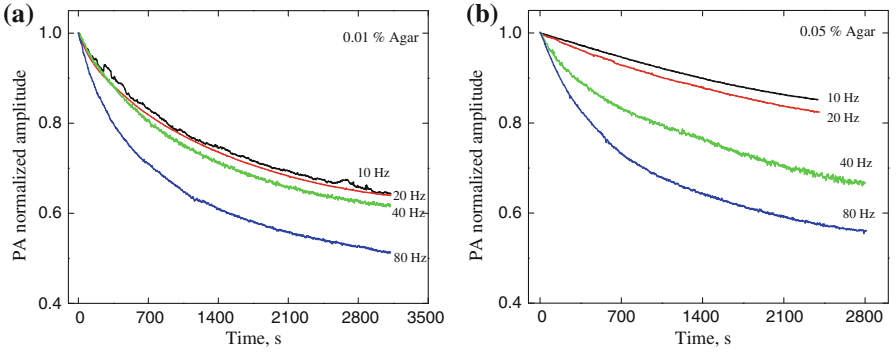


**Fig. 4** Normalized photoacoustic signal for (**a**) 0.01 % and (**b**) 0.05 % w/v of agar

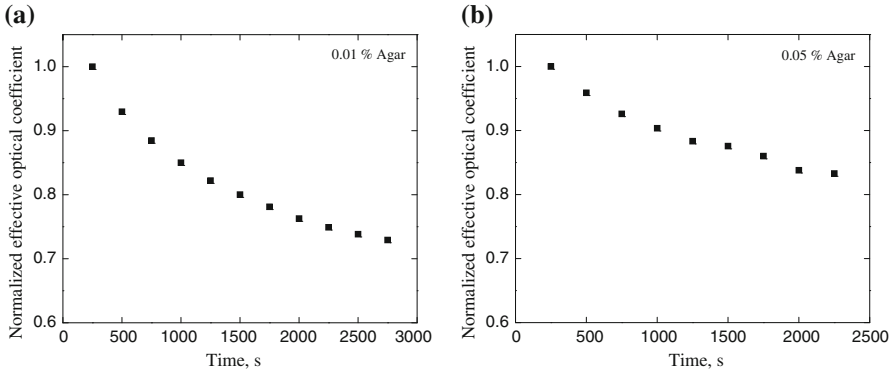


**Fig. 5** Normalized effective optical absorption coefficient as a function of time, for two gel phantoms with concentrations (**a**) 0.01 % and (**b**) 0.05 % w/v of agar during the dye diffusion

agar samples in which the dye solution was completely diluted did not show considerable differences with the samples without the dye, being $1.453\times10^{-7}\,\mathrm{m}^2\cdot\mathrm{s}^{-1}$ and $1.455\times10^{-7}\,\mathrm{m}^2\cdot\mathrm{s}^{-1}$ for 0.01 % and 0.05 % w/v agar concentrations, respectively. Using these values, considering the changes in the thermal diffusivity of agar due to the addition of the dye, a simulation process of Eq. 10 was performed. It was found that they do not affect appreciably the magnitude of the PA signal. Therefore, the influence of the dye solution and its diffusion inside the agar gel on the thermal diffusivity values can be considered negligible. Based on these results, the changes in the PA signal can be exclusively related to changes of the optical properties of the sample and can be appropriately parameterized as an effective optical absorption coefficient $\beta_{\mathrm{eff}}$, that would measure the light that is being converted into heat during the diffusion process. Experimental data shown in Fig. 4 were fitted with Eq. 12, considering the thermal diffusivity values measured using the thermal wave resonator for the agar and gel mentioned above, thermal effusivity $\varepsilon_2 = 1588\,\mathrm{W}\cdot\mathrm{s}^{1/2}\cdot\mathrm{m}^{-2}\cdot\mathrm{K}^{-1}$, and for the polyvinyl acetate, $\alpha_1 = 1.95\times10^{-7}\mathrm{m}^2\cdot\mathrm{s}^{-1}$ and $\varepsilon_1 = 490\,\mathrm{W}\cdot\mathrm{s}^{1/2}\cdot\mathrm{m}^{-2}\cdot\mathrm{K}^{-1}$. With this procedure, the values of the effective optical absorption coefficients are obtained, as shown in Fig. 5.

The effective absorption coefficient shows a systematic decay on a time scale of 1,000 s for both samples. In order to get usable numerical data, a fitting procedure can be performed using an exponential decay, parameterized in the form,

$$y = y_0 + A_1 e^{-(t-t_0)/\tau} \tag{13}$$

where $t$ is the time, $y_0$ is the value of the absorption coefficient when the time is very large, $A_1$ measures the size of the decay of the absorption, $t_0$ is the initial time, and $\tau$ is the characteristic time decay of the process that measures the time interval needed in the process of dilution for the methylene blue solution in the agar sample to stabilize. The characteristic decay times for the 0.01 % and 0.05 % w/v agar samples are 1,111 s and 1,232 s, respectively. This can be understood taking into account that when the concentration of agar grows, the agar gel becomes harder; therefore, it is more difficult for methylene blue to penetrate the solution. We showed first that the technique is sensitive and useful in the measurement of this time, and second, it provides the difference in time in which the methylene blue solution diffuses for two agar concentrations. These differences supply important results for biomedical sciences in which agar gels are used as phantoms resembling some of the properties of living organs and tissues.

This work shows that when the concentration of agar in water is increased by a factor of five, the stabilization time only grows around 10 %; this behavior is expected to occur only at low agar concentrations. At higher agar concentrations, stabilization of the processes would take longer time intervals. At these concentrations, the bond among the agar molecules generates a strong structure that is harder to penetrate by the dye [1].

The diffusion process of diluted methylene blue in the phantom, registered by purely optical detection is shown in Fig. 6. The absorption peak falls as a consequence of the systematic diffusion of the methylene blue, after the cell has been put upside down to allow the migration of the methylene blue solution. In this case, the diffusion can be observed during the whole process, since the solid is not attached to any wafer and, consequently, the liberation is immediate.

## 5 Conclusions

It has been shown that the PA technique has allowed monitoring of the diffusion process of a dye, in this case, methylene blue, inside an agar phantom sample. The process was observed as the sudden growth of the PA signal amplitude followed by a long and systematic decay. This is related to the gradual diffusion of the dye inside the gel. A simple theoretical approach allowed us to relate the changes in the PA signal with the time evolution of an effective optical absorption coefficient. These values were fitted using first-order kinetics equation that provided a characteristic time, which measures the temporal interval of the stabilization of the dye diffusion process inside the agar matrix. Our results also show that higher agar concentrations require longer stabilization time intervals to settle down.

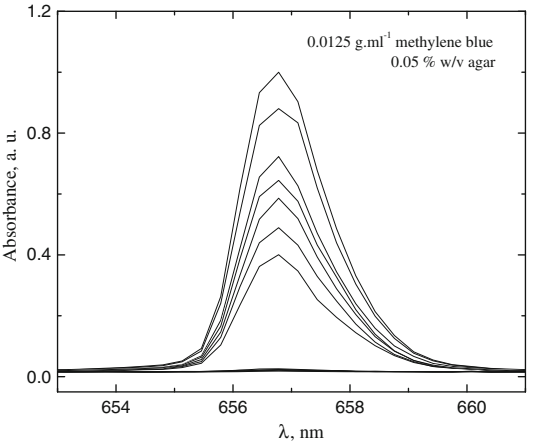


**Fig. 6** Time evolution of the absorption spectra of the methylene blue solution inside of an agar gel. Each pair of successive spectra corresponds to a time interval of one second

**Acknowledgments** This work was partially supported by the CONACYT 49275-F (24214), 105816, Multidisciplinary-Cinvestav 2009, FOMIX No.108160, 108528 and Foncicyt 96095 projects. The authors want to express their acknowledgments to M.S. J. Bante and M.S. D. Aguilar, for their valuable help in the cells and electronic construction.

## References

1. E. Madsen, M. Hobson, H. Shi, T. Varghese, G. Frank, Phys. Med. Biol. **50**, 5597 (2005)
2. M. Bauman, G. Gillies, R. Raghavan, M. Brady, C. Pedain, Nanotechnology **15**, 92 (2004)
3. M. Staples, K. Daniel, J. Michael, R. Langer, Pharm. Res. **23**, 5 (2006)
4. K. Buchholz, A. Marcelo, D. Wissenbach, H. Schirmer, L. Krauth-Sieguel, S. Gromer, Mol. Biochem. Parasitol. **160**, 65 (2008)
5. D. Almond, P. Patel, in *Photothermal Science and Techniques, Physics and its Applications*, ed. by E.R Dobbs, S.B. Palmer (Chapman and Hall, London, 1996)
6. A. Mandelis, in *Non-Destructive Evaluation: Progress in Photothermal and Photoacoustic Science and Technology*, vol. 2 (PTR Prentice Hall, Englewood Cliffs, NJ, 1993)
7. H. Vargas, L.C.M. Miranda, Phys. Rep. **161**, 43 (1988)
8. D. Acosta-Avalos, J.J. Alvarado-Gil, H. Vargas, J. Frías-Hernández, V. Olalde-Portugal, L.C.M. Miranda, Plant Sci. **119**, 183 (1996)
9. A. Frandas, D. Paris, C. Bissieux, M. Chirtoc, J.S. Antoniow, M. Egée, Appl. Phys. B **71**, 69 (2000)
10. A. Landa, J.J. Alvarado-Gil, J. Gutiérrez-Juárez, M. Vargas-Luna, Rev. Sci. Instrum. **74**, 377 (2003)
11. P. Martínez-Torres, J.J. Alvarado-Gil, Int. J. Thermophys. **28**, 996 (2007)
12. S.E. Bialkowski, in *Photothermal Spectroscopy Methods for Chemical Analysis* (John Wiley & Sons, Inc., New York, 1996)
13. N.C. Fernelius, J. Appl. Phys. **51**, 1756 (1980)
14. R. Quimby, W.J. Yen, J. Appl. Phys. **51**, 1780 (1980)
15. Y.C. Teng, B.S.H. Royce, J. Opt. Soc. Am. B **70**, 557 (1980)
16. G.C. Wetsel Jr., F.A. McDonald, Appl. Phys. Lett. **30**, 252 (1977)
17. M. Vargas-Luna, G. Gutiérrez-Juárez, J.M. Rodríguez-Vizcaíno, J.B. Varela-Nájera, J.M. Rodríguez-Palencia, J. Bernal-Alvarado, M. Sosa, J.J. Alvarado-Gil, J. Phys. D Appl. Phys. **35**, 1532 (2002)
18. J. Shen, A. Mandelis, Rev. Sci. Instrum. **66**, 10 (1995)
19. A. Matvienko, A. Mandelis, Rev. Sci. Instrum. **77**, 064906 (2006)
20. H.S. Carslaw, in *Introduction to the Theory of Fourier's Series and Integrals* (University of Michigan, Ann Arbor, MI, 2005)
21. J.L. Pichardo, J.J. Alvarado-Gil, J. Appl. Phys. **89**, 4070 (2001)